NRIAG JOURNAL OF ASTRONOMY AND GEOPHYSICS
2019, VOL. 8, NO. 1, 97–102
https://doi.org/10.1080/20909977.2019.1615804

A new model for reduction of Azimuth asymmetry biases of tropospheric delay

A. Nabil[a], M. A. Abdelfatah[a], A. E. Mousa[b] and G. S. El-Fiky[a]

[a]Construction Department & Utilities, Faculty of Engineering, Zagazig University, Zagazig, Egypt; [b]Geodynamic Department, Crustal Movement Lab, National Research Institute of Astronomy & Geophysics, Helwan, Egypt

ABSTRACT

Nowadays, a GNSS application is one of the main backbones of lifestyle. The GNSS signal that comes from space satellites to receivers on Earth suffers some delays. The troposphere layer is one of the basic sources of delay to signals. To detect the delay, many models have been produced taking into account the receiver location and satellite zenith angle. Most of these models give vertically perfect representation without accounting the horizontal asymmetry effect. The horizontally graded difference "azimuth asymmetry" is negligible at high elevation angles up to 10°. At low elevation angles, the asymmetry is significant. At 2° elevation angle, the asymmetry is about 72 mm for east and west and about 66 mm for south. Using the Precise Tropospheric Delay Database (PTD), the difference in horizontal plane delays is studied. A new model is proposed and compared to PTD calculations. The model has three coefficients obtained for high zenith angles (70° to 88°). These coefficients are modelled as a function of zenith angle and used to give a horizontal gradient factor which is multiplied by the northern mapping function to map it to any azimuth. The proposed model makes significant improvement. For east and west directions, the model decreases the bias from around 72 mm to be about 1.0 mm. For the southern direction, the produced model needs an improvement to get closer to the true asymmetry.

Abbreviations: GNSS: Global Navigation Satellite Systems; HG: Horizontal Gradient; MF: Mapping Function; PTD: Precise Tropospheric Delay Database; Z: Zenith Angle; ZHD: Zenith Hydrostatic Delay; ZTD: Zenith Total Delay; ZWD: Zenith Wet Delay

KEYWORDS

Troposphere delay; Azimuth asymmetry; horizontal gradient

1. Introduction

GNSS applications have become very essential for all life branches. Most of the world needs are related to these applications somehow. Being on that high level of importance makes it necessary to focus on assessment and development. Satellites send continuous signals to GNSS receivers which analyse these signals to give a precise position. This precision is contaminated by some errors. Satellite clock, receiver clock, multipath, antenna phase centre and atmosphere are the most serious error sources.

The atmosphere affects signals by two consecutive layers; Ionosphere and Troposphere. Although the ionosphere effect is greater in value than the troposphere effect, it is less dangerous because it can be almost eliminated by using dual-frequency observations (e.g. Herring 1983; Brunner, 1991). In the case of active ionosphere, the ionospheric delay can be over 100 m, which has a great impact on the positioning accuracy of single-frequency GNSS users (Chen and Guo 2018).

Zenith troposphere delay ranges between 2.30 and 2.60 m (e.g. Elsobeiey and El-diasty 2016). To get over this error, numerical models as well as databases are produced to improve the positioning accuracy as much as possible. Previous models focused on the elevation/zenith angle and were concluded in all models as a main factor.

The dry delay caused by the troposphere layer at the zenith direction is approximately 2.4 m while at Z = 88° the delay is about 40 m (e.g. Abdelfatah 2015). On the contrary, the fluctuation in the dry delay among different azimuths is about 10.3 cm (Abdelfatah 2015). Ignoring the azimuthal asymmetry of the neutral atmosphere may result in a negative influence on the high precision of GNSS applications (Ge and Schuh 2016). The ZTD (Zenith Total Delay) models provide only vertically integrated information on the atmospheric refractivity, whereas the information in connection with horizontal atmospheric distribution is not considered. To account for the horizontal variation of refractivity in the troposphere, atmospheric gradients were introduced (e.g. MacMillan 1995).

In the current study, the azimuth asymmetry (Figure 1) effect is on spot. A 30° step azimuth in front of 5 zenith angles (70, 80, 84, 86, 88) is evaluated to detect their effect. In addition, a new model is developed to calculate the satellite azimuth effect and

CONTACT A. Nabil ahmednabel@zu.edu.eg Construction Department & Utilities, Faculty of Engineering, Zagazig University, Zagazig, Egypt

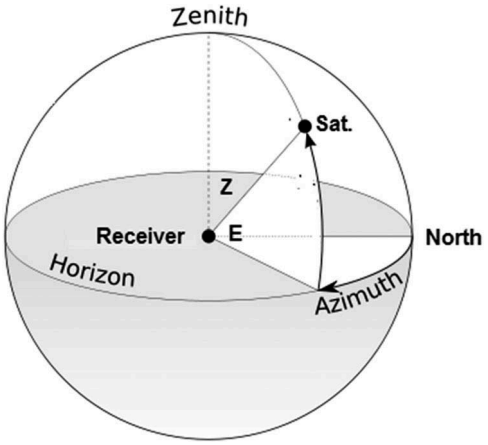

Figure 1. Satellite Azimuth and elevation angle.

reduce its bias on dry tropospheric delay for low elevation angles.

2. Analysis of previous models

The tropospheric delay gradient models such as (MacMillan 1995) expresses the delay as a sum of the mapped total delay and horizontal gradients. Chen and Herring (1997) proposed a mathematical model to compute the total slant tropospheric delay (T) including the dry and wet parts of the troposphere as well as the horizontal gradient:

$$T = MF_h * ZHD + MF_w * ZWD + M_G(G_{ns}\cos\alpha + G_{ew}\sin\alpha) \quad (1)$$

MF_h is the hydrostatic mapping function, MF_w is the wet mapping function.ZHD refers to zenith hydrostatic delay while ZWD refers to zenith wet delay. α indicates satellite azimuth. $G_{ns}$and $G_{ew}$are the north-south and east-west horizontal gradients, respectively. M_G is the gradient mapping function.

The zenith tropospheric delay can be calculated using an empirical model such as Saastamoinen (1973). $G_{ns}$and G_{ew}can be calculated depending on the horizontal gradient refractivity components for the north-south direction (N_{ns}) and the east-west direction (N_{ew}) integrated by the height (h) above the observation site as (Chen and Herring 1997):

$$G_{ns} = 10^{-6} \times \int_0^H N_{ns} h dh \quad (2)$$

$$G_{ew} = 10^{-6} \times \int_0^H N_{ew} h dh \quad (3)$$

The gradient mapping function M_G is computed by the next equation where E is the elevation angle and C is a constant. In geodetic analyses, we usually use C = 0.0032 (Herring 1992)

$$M_G = \frac{1}{\sin(E)\tan(E) + C} \quad (4)$$

Davis et al. (1993) assume that the linear horizontal gradients G can be determined (Equation 5) for a specific azimuth α if the refractivity gradient $dN\alpha$ is known for the neutral atmosphere at any height z above the site and that $dN\alpha$ is valid at any horizontal distance d around the vertical profile (Boehm and Schuh 2007).

$$G_\alpha = 10^{-6} \times \int_{z=0}^{\infty} dN\alpha(z) z dz \quad (5)$$

In addition, the horizontal gradient (HG) has the following form of the International Earth Rotation and Reference Systems Service (IERS Conventions 2010)

$$HG = [G_N cos(\alpha) + G_E sin(\alpha)]M_G \quad (6)$$

G_N and G_E are the northern and eastern horizontal delay gradients, respectively. α is the satellite azimuth angle.

Abdelfatah et al. (2015) studied the azimuth asymmetry effect. Metrological data of 10 radiosonde stations through and around Egypt are used to get the troposphere slant delays through a ray tracing process. They concluded that the delay for both east and west directions is approximately the same while the delay for south is greater than the corresponding delay for north by about 10.3 cm as an average for the dry case. For the wet case, the fluctuation is found to be about 7.1 cm among different seasons of the year.

3. Data collection and analysis procedure

The proposed model is a second-degree polynomial model. The satellite azimuth is the master parameter. It consists of three coefficients a, b and c. Each coefficient is computed through a similar second-degree polynomial equation depending on satellite zenith angle. After the computation of the coefficients listed before, the horizontal gradient factor is the outcome of the equation. As delay error may reach 77 mm at Z = 88° if azimuth asymmetry is ignored, the target of proposing the model is to improve precision and reduce errors as much as possible.

The main source of the study data is PTD Database introduced by Abdelfatah (2015). This database is built on the metrological data that come from 10 radiosonde stations distributed in and around Egypt. A ray tracing technique is applied to provide a zenith delay and slant delays at different zenith angles for both dry and wet parts of the troposphere. Also the azimuth can be applied at the database to compute the delay difference in the horizontal plane. The final data collected for analysis are a zenith delay and slant delays for the following different zenith angles 70°, 80°, 84°, 86° and 88°. These delays are computed for a grid of 36 points in Egypt. This grid ranges in latitudes from 22° to 32°, and in longitudes

Figure 2. The 36 grid points cover Egypt used to compute the zenith delay and the slant delays (Abdelfatah et al. 2015).

from 25° to 35° with a 2° increment in each direction (Figure 2). Besides, all the delays were repeated for azimuths from 30° to 330° with an interval of 30°. Data are collected for the 366 days of the year 2016.

For each case of the collected data, a mapping function is extracted by the division of the slant delay by the corresponding zenith delay. Note that here the geometric delay is excluded. For each azimuth and each zenith angle, a separate mapping function is computed for average latitudes and longitudes.

Assuming the following equation for the calculation of the horizontal gradient factor (HG), a least square analysis is applied.

$$\mathrm{HG} = \mathrm{a}\cos^2(\alpha) + \mathrm{b}\cos(\alpha) + \mathrm{c} \tag{7}$$

Where α is the satellite azimuth. Least square process aims to obtain the coefficient values as a function of zenith (Z). These values are evaluated for each zenith angle under study. The horizontal gradient factor is multiplied by the northern mapping function to obtain a new mapping function at any satellite azimuth. For coefficient values, the following equations are applicable:

$$a = a_1 cos^2 Z + a_2 \cos Z + a_3 \tag{8}$$

$$b = b_1 cos^2 Z + b_2 \cos Z + b_3 \tag{9}$$

$$c = c_1 cos^2 Z + c_2 \cos Z + c_3 \tag{10}$$

Table 1. Sub-coefficient values (a_i,b_i, c_i).

	f_1	f_2	f_3
a_i	−0.110,588	0.033613	−0.002712
b_i	0.019825	−0.004248	−0.000029
c_i	0.090235	−0.029199	1.002727

Sub-coefficient values (f_i) for the last three polynomial equations are expanded in Table 1.

4. Results and discussion

4.1. According to Azimuth

The produced coefficients a, b and c can be used beside the satellite azimuth to get the horizontal gradient factor (HG). A numerical comparison is set between three cases; (i) the remaining difference calculated by the PTD database when ignoring the horizontal gradient effect, (ii) the remaining difference after applying the model of Chen and Herring (1997), and (iii) the error remains after applying the new model proposed here. The comparison is built upon the slant delay error differences between these cases at different zenith angles (80° to 88°) and for different azimuths (30° to 330°). Shown numbers in front of each azimuth is the test days' average. Test days are 35 days selected from 2015 representing all months as the first three days of each month.

Table 2 shows delay errors to be less than 10 mm in most cases which mean that at Z = 80° the horizontal

Table 2. Slant delay error differences (mm) between the three studied cases in front of Azimuth at Z = 80°.

Azimuth	None		Chen and Herring		New Model	
	Mean	RMS	Mean	RMS	Mean	RMS
30	0.80	0.54	6.78	0.54	0.08	0.53
60	3.22	2.04	4.35	2.04	0.37	2.02
90	6.06	4.00	0.51	4.00	1.59	3.98
120	8.13	5.85	6.10	5.85	3.28	5.84
150	9.22	6.98	7.19	6.98	4.88	6.98
180	9.45	7.32	3.91	7.32	5.47	7.32
210	8.97	6.88	1.39	6.88	4.63	6.89
240	7.77	5.77	0.19	5.77	2.92	5.76
270	5.95	3.99	0.40	3.99	1.48	3.97
300	3.52	2.09	1.49	2.09	0.67	2.07
330	1.17	0.61	0.86	0.61	0.29	0.60
Average	5.84	–	3.02	–	2.33	–

Table 5. Slant delay error differences (mm) between the three studied cases in front of Azimuth at Z = 88°.

Azimuth	None		Chen and Herring		New Model	
	Mean	RMS	Mean	RMS	Mean	RMS
30	7.83	4.54	16.94	4.43	8.82	4.29
60	41.69	21.02	16.91	20.92	9.53	20.00
90	72.44	39.62	54.29	39.52	2.07	38.19
120	77.73	49.91	71.07	49.84	20.60	48.93
150	68.19	52.69	61.58	52.64	41.30	52.59
180	65.67	51.70	47.55	51.54	54.19	51.79
210	62.01	49.98	37.24	49.78	35.12	50.11
240	64.47	46.19	39.69	45.95	7.34	45.53
270	71.56	39.28	53.41	39.18	1.19	37.87
300	59.40	22.97	52.74	22.93	8.19	21.89
330	26.07	6.51	19.46	6.49	9.42	6.10
Average	56.10	–	42.81	–	17.98	–

gradient is not significant and can be neglected. Chen and Herring model has an average error of 3.02 mm while the new model has an average error of 2.33 mm that makes it slightly preferred.

Table 3 represents the delay differences at Z = 84°. Delays are greater than the previous case of Z = 80° and are more considerable. The case of ignoring horizontal gradient effect is the worst at all azimuths then the model of Chen and Herring and the best at all cases is the new model with an average error of 14.39, 8.90 and 5.19 mm, respectively.

At Z = 86°, the delay error crosses 35 mm at α = 120° according to PTD. The effect is clear and noticeable. The ignoring case is the worst at all azimuths except at α = 30° where Chen and Herring model is worse. The new model shows the least errors at all azimuths. The average error results for the three cases are 26.22 mm for the ignoring case, 17.71 mm for Chen and Herring model and 8.39 mm for the new model (Table 4).

At the lowest elevation angle; Z = 88° where delays are the highest (Table 5), a fluctuation from 7.83 mm to 77.73 mm takes place according to PTD calculations. Delays get bigger as the azimuth angle increases towards the east direction, then decreases again moving to the south and go higher to the west, down again back to the north. Eastern and western delay components are approximately the same (72.44 and 71.56 mm, respectively). On the contrary, northern and southern delay components have a 65.67 mm difference.

The new model shows a great performance especially at the east and west directions. At all other azimuths, the new model is preferred except at South where Chen and Herring model has a less error. The average error for the three cases is 56.10 mm for the ignoring case, 42.81 mm for Chen and Herring model, and 17.98 mm for the new model.

Table 3. Slant delay error differences (mm) between the three studied cases in front of Azimuth at Z = 84°.

Azimuth	None		Chen and Herring		New Model	
	Mean	RMS	Mean	RMS	Mean	RMS
30	2.05	1.28	9.83	1.28	0.43	1.26
60	8.71	4.97	3.18	4.98	0.70	4.90
90	15.95	9.64	7.24	9.64	3.67	9.55
120	20.19	13.80	17.00	13.80	7.42	13.75
150	21.41	16.34	18.23	16.34	10.68	16.34
180	21.43	16.79	12.73	16.79	11.96	16.81
210	20.47	15.92	8.59	15.92	9.75	15.94
240	18.69	13.63	6.80	13.62	5.92	13.61
270	15.68	9.58	6.97	9.58	3.40	9.50
300	10.08	5.28	6.89	5.28	2.07	5.19
330	3.61	1.66	0.43	1.67	1.13	1.63
Average	14.39	–	8.90	–	5.19	–

Table 4. Slant delay error differences (mm) between the three studied cases in front of Azimuth at Z = 86°.

Azimuth	None		Chen and Herring		New Model	
	Mean	RMS	Mean	RMS	Mean	RMS
30	3.84	2.26	12.46	2.26	2.58	2.21
60	17.27	9.17	0.96	9.18	2.84	8.94
90	30.93	17.51	18.98	17.50	2.14	17.22
120	36.99	24.27	32.62	24.26	11.07	24.10
150	36.53	28.33	32.16	28.32	20.01	28.31
180	35.63	28.60	23.69	28.56	24.11	28.63
210	34.18	27.34	17.88	27.30	17.67	27.37
240	33.19	23.68	16.88	23.65	7.26	23.59
270	30.46	17.37	18.51	17.36	1.67	17.09
300	21.15	10.27	16.77	10.27	1.05	9.99
330	8.30	3.00	3.94	3.01	1.88	2.90
Average	26.22	–	17.71	–	8.39	–

4.2. According to day of year

For Z = 88° and whereas delay differences are most significant, next graphs show briefly a comparison between the previous cases for east, west, and south in front of the north direction's slant delays (Figures 3–5). At the figures, the error of the ignoring case detected by PTD calculations is compared to the remaining error after using both models; the new model and Chen and Herring model. Calculations are expanded horizontally for the 35 tested days of the year 2015.

Figures (3–5) show the large fluctuation of azimuth asymmetry among year days according to PTD calculations. For the eastern and western directions (Figures 3 and 4), the model improves results and gives less errors than the cases of ignoring and Chen and Herring model. For the southern direction (Figure 5), the three cases give approximately the same delay. The new model needs more adjustment to improve its accuracy while simulating azimuth asymmetry for the south direction.

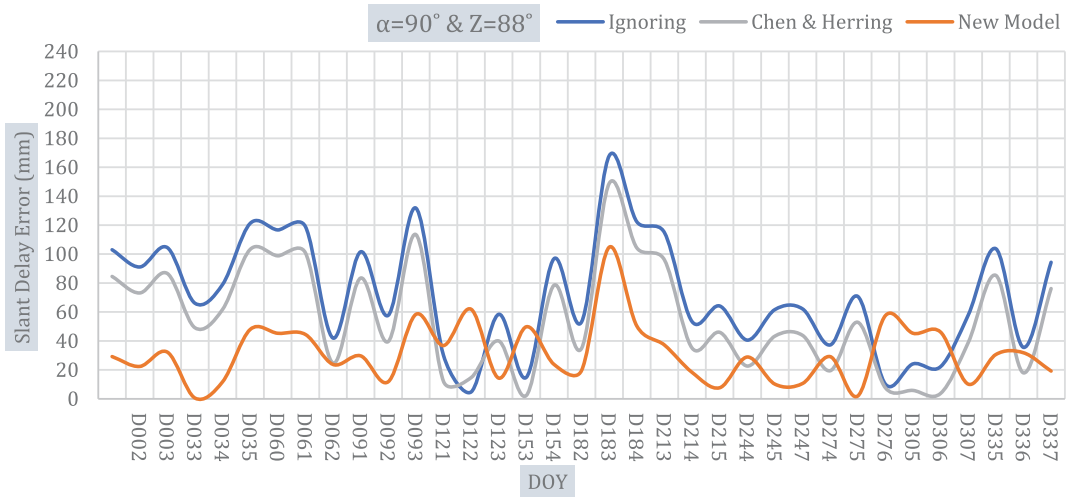

Figure 3. A slant delay error comparison of the eastern direction to the northern direction at Z = 88°.

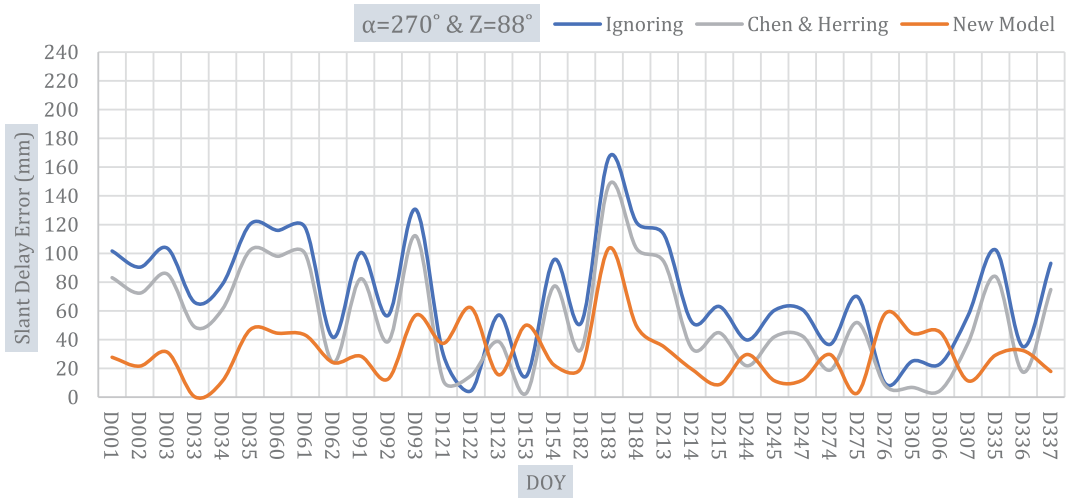

Figure 4. A slant delay error comparison of the western direction to the northern direction at Z = 88°.

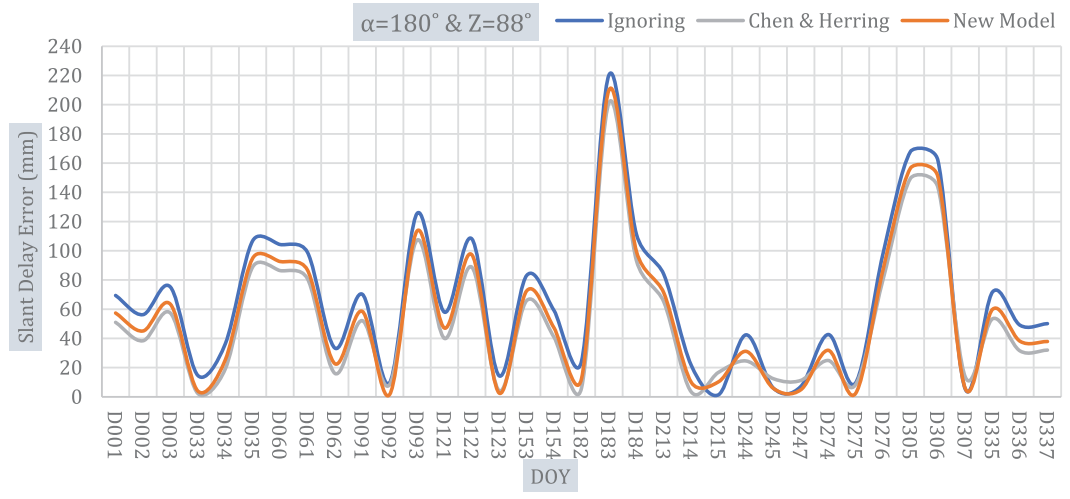

Figure 5. A slant delay error comparison of the southern direction to the northern direction at Z = 88°.

5. Conclusions

The Precise Tropospheric Delay Database (PTD) has been used to study the graded difference in horizontal plane delays. A new model has been proposed and compared to PTD calculations. The new model is based on the analysis of a whole year data (2016). Testing is performed over 35 days of the year (2015) regularly distributed to represent all the months. The model contains three coefficients (a, b and c) obtained for high zenith angles (70°, 80°, 84°, 86° and 88°). Coefficients are introduced as a function of zenith angle. These coefficients compute a horizontal gradient factor able to map the northern mapping function to any azimuth.

Obtained results indicated the horizontal gradient effect to be negligible for high elevation angles down to elevation angle of 10°. The maximum slant delay difference all over all azimuths, other than north, is 9.45 mm with an average of 5.84 mm. The delay difference increases with low elevation angles (6°, 4° and 2°) where the effect is noticeable. At Z = 88°, the maximum slant delay difference is 77.73 mm with an average of 56.10 mm for all azimuths.

As for the horizon, the delay difference due to horizontal gradient effect starts with a small value at α = 30°. It increases gradually to be maximum at α = 90° and α = 270°. Between these two values, it gets back to decrease at α = 180°, in most cases. The delay difference at α = 30° is found to be less than the difference at α = 330°. The delay difference α = 60° is less than that of α = 300° while the eastern and western directions (α = 90° and α = 270°) have approximately the same effect. Differences at α = 120° and α = 150° are greater than α = 240° and α = 210°, respectively.

Compared to cases of ignoring and Chen and Herring model, the new model reduces the biases vitally for all azimuths except the southern direction where the three models give approximately the same delay.

Disclosure statement

No potential conflict of interest was reported by the authors.

References

Abdelfatah MA (2015). Database for precise troposphere delay model for Egypt, as derived from radiosonde data [Faculty of Engineering, Ph.D. Thesis]. Egypt: Zagazig University.

Abdelfatah MA, Mousa AK, ElFiky G. 2015. Precise troposphere delay model for Egypt, as derived from radiosonde data. NRIAG J Astron Geophys. 4(1):1–9.

Boehm J, Schuh H. 2007. Troposphere gradients from the ECMWF in VLBI analysis. J Geodesy. 81(6–8):403–408. doi:10.1007/s00190-007-0144-2.

Brunner FK, MG. 1991. An improved model for the dual frequency ionospheric correction of GPS observations. Geod. 16:205–214.

Chen G, Herring TA. 1997. Effects of atmospheric azimuth asymmetry on the analysis of space geodetic data. J Geophys Res. 102(B9):20489–20502. doi:10.1029/97JB01739.

Chen L, Guo H, (2018). A precise regional ionospheric model was established based on GNSS technique. China Satellite Navigation Conference. doi:10.1007/978-981-13-0014-1_53.

Davis JL, Elgered G, Niell AE, Kuehn CE. 1993. Ground-based measurements of the gradients in the 'wet' radio refractivity of air. Radio Sci. 28(6):1003–1018.

Elsobeiey M, El-diasty M. 2016. Impact of tropospheric delay gradients on total tropospheric delay and precise point positioning. Int J Geosci. 2016(May):645–654.

Ge M, Schuh H. 2016. GNSS tropospheric gradients with high temporal resolution and their effect on precise positioning. J Geophys Res. 912–930. doi:10.1002/2015JD024255.Received.

Herring TA. 1983. The precision and accuracy of intercontinentaldistance determinations using radio interferometry. Cambridge. [Ph.D. Thesis]. Massachusetts Institute of Technology, Dept. of Earth and Planetary Sciences

Herring TA. 1992. Modeling atmospheric delays in the analysis of space geodetic data. In: Munck JC DE, Spoelstra TA, editors. Netherlands geodetic commission publications in geodesy. Vol. 86. 157–164

IERS Conventions. 2010. International earth rotation and reference systems service. [accessed 2018 May 21]. https://www.iers.org/IERS/EN/Publications/TechnicalNotes/tn36.html.

MacMillan D. 1995. Atmospheric gradients from very long baseline interferometry observations. J Geophys Res. 22 (9):1041–1044.

Saastamoinen J. 1973. Contribution to the theory of atmospheric refraction. Nat Res Counc Canada. 107 (45):13–34.